

## Article

# Mitochondrial Translation Occurs Preferentially in the Peri-Nuclear Mitochondrial Network of Cultured Human Cells

Christin A. Albus <sup>1,\*</sup>, Rolando Berlinguer-Palmini <sup>2</sup>, Caroline Hewison <sup>3</sup>, Fiona McFarlane <sup>3</sup>,  
Elisabeta-Ana Savu <sup>3</sup>, Robert N. Lightowlers <sup>1</sup>, Zofia M. Chrzanowska-Lightowlers <sup>1</sup> and Matthew Zorkau <sup>1,\*</sup>

<sup>1</sup> Wellcome Centre for Mitochondrial Research, Biosciences Institute, Faculty of Medical Sciences, Newcastle University, Newcastle upon Tyne NE2 4HH, UK; Robert.Lightowlers@ncl.ac.uk (R.N.L.); Zofia.Chrzanowska-Lightowlers@ncl.ac.uk (Z.M.C.-L.)

<sup>2</sup> Bioimaging Unit, Faculty of Medical Sciences, Newcastle University, Newcastle upon Tyne NE2 4HH, UK; rolando.berlinguer-palmini@newcastle.ac.uk

<sup>3</sup> School of Biomedical, Nutritional, and Sport Sciences, Newcastle University, Newcastle upon Tyne NE2 4HH, UK; c.l.hewison@newcastle.ac.uk (C.H.); F.McFarlane@newcastle.ac.uk (F.M.); E.Savu@newcastle.ac.uk (E.-A.S.)

\* Correspondence: Christin.Albus@newcastle.ac.uk (C.A.A.); Matthew.Zorkau@newcastle.ac.uk (M.Z.); Tel.: +44-191208-8454 (C.A.A. & M.Z.)



**Citation:** Albus, C.A.; Berlinguer-Palmini, R.; Hewison, C.; McFarlane, F.; Savu, E.-A.; Lightowlers, R.N.; Chrzanowska-Lightowlers, Z.M.; Zorkau, M. Mitochondrial Translation Occurs Preferentially in the Peri-Nuclear Mitochondrial Network of Cultured Human Cells. *Biology* **2021**, *10*, 1050. <https://doi.org/10.3390/biology10101050>

Academic Editor: Jukka Finne

Received: 11 August 2021

Accepted: 12 October 2021

Published: 15 October 2021

**Publisher's Note:** MDPI stays neutral with regard to jurisdictional claims in published maps and institutional affiliations.



**Copyright:** © 2021 by the authors. Licensee MDPI, Basel, Switzerland. This article is an open access article distributed under the terms and conditions of the Creative Commons Attribution (CC BY) license (<https://creativecommons.org/licenses/by/4.0/>).

**Simple Summary:** All the cells in our bodies need energy to survive. This chemical energy is generated by a subcompartment of the cell called the mitochondrial network. The complexes that generate this cellular fuel, require 13 protein components to be synthesised inside this mitochondrial network. Our project looked to see whether the manufacture of these protein components was evenly distributed within the network. We identified that there is a gradient of activity that is highest near the nucleus and diminishes towards the edges of the cell and that this did not seem to be caused by a lack of the machinery responsible for the protein synthesis. This work is important because it now allows us to use this newly refined technology to investigate whether this pattern changes in patients with mitochondrial disorders. These are a group of diseases that cause malfunctions in muscle, brain, nerve and other tissues that get progressively worse with time and which are currently untreatable. A deeper understanding of what has gone wrong may help us understand the disease process better, with a longer-term view of treating the disorders.

**Abstract:** Human mitochondria are highly dynamic organelles, fusing and budding to maintain reticular networks throughout many cell types. Although extending to the extremities of the cell, the majority of the network is concentrated around the nucleus in most of the commonly cultured cell lines. This organelle harbours its own genome, mtDNA, with a different gene content to the nucleus, but the expression of which is critical for maintaining oxidative phosphorylation. Recent advances in click chemistry have allowed us to visualise sites of mitochondrial protein synthesis in intact cultured cells. We show that the majority of translation occurs in the peri-nuclear region of the network. Further analysis reveals that whilst there is a slight peri-nuclear enrichment in the levels of mitoribosomal protein and mitochondrial rRNA, it is not sufficient to explain this substantial heterogeneity in the distribution of translation. Finally, we also show that in contrast, a mitochondrial mRNA does not show such a distinct gradient in distribution. These data suggest that the relative lack of translation in the peripheral mitochondrial network is not due to an absence of mitoribosomes or an insufficient supply of the mt-mRNA transcripts.

**Keywords:** mitochondria; mammalian; protein synthesis; heterogeneity; co-localisation; peri-nuclear; peripheral

## 1. Introduction

Mitochondria are organelles found in virtually all eukaryotes and all nucleated cells in the human body. They are integral to numerous functions such as the intrinsic pathway

of apoptosis, generating Fe-S clusters as cofactors for important proteins and housing the enzymes responsible for pathways of oxidative metabolism. Central to the latter function is the formation of five key multi-subunit enzyme complexes that together couple cellular respiration to the production of ATP. This process is termed oxidative phosphorylation (OXPHOS) and it is the terminal step in oxidative metabolism. Four of these five complexes share a unique feature in that they contain components that are encoded by the mitochondrial genome (mtDNA), which are translated within the mitochondrial matrix. Consequently, mitochondrial gene expression is essential for cell viability.

Although original studies were interpreted to suggest that mammalian mitochondria formed many discrete organelles in the cytoplasm of the cell, more recent work has shown very clearly that mitochondria in nearly all cell types form dynamic networks, fusing and budding in a process that is choreographed by a handful of well-described proteins [1]. Within the network, the inner mitochondrial membrane has large numbers of infoldings or cristae that are also remarkably dynamic, extending into the matrix and harbouring the majority of the OXPHOS supercomplexes [2–4]. The inner membrane can therefore be considered as having two discrete domains, the inner boundary membrane that parallels the outer membrane and the infoldings that constitute the cristae membranes. The two are retained as distinct by cristae junctions that largely comprise the MICOS and associated proteins [5]. This internal architecture has been suggested to isolate subcompartments, such that cristae within the same section of a mitochondrial network can support disparate membrane potentials, reflecting a heterogeneous bioenergetic status within a single network [6].

Our understanding of mitochondrial gene expression has grown enormously in recent years [7,8]. Mitochondrial DNA is condensed to form many discrete nucleoids in the network [9–11]. This relatively short (~16.5 kb) molecule is transcribed virtually in its entirety from both strands to form polycistronic RNA units that are processed and matured in RNA granules [12,13] that are found close to the nucleoids [14,15]. The resultant mature RNAs are then assembled into mitoribosomes (mt-rRNAs and a subset of mt-tRNA<sup>Val</sup>), aminoacylated (mt-tRNAs) or translated (mt-mRNAs).

Protein synthesis is essentially the last step of gene expression and the process of oxidative phosphorylation that culminates in the generation of ATP requires the synthesis of all 13 proteins that are encoded in the human mtDNA [16]. The molecular machine responsible for intramitochondrial translation is the mitoribosome, which is made up of the small (mt-SSU) and large (mt-LSU) subunits comprising ~80 proteins [17] all of which are encoded by the nuclear genome, together with two mtDNA encoded ribosomal rRNAs (*RNR1* and *RNR2*) and the *mt-tRNA<sup>Val</sup>* that takes the place of the 5S rRNA in the large subunit [18]. Unlike for transcription, processing and maturation, the exact submitochondrial locale of actively translating mitoribosomes has, until recently, not been clear.

By exploiting the technique of click chemistry in a process termed mitochondrial FUNCAT (*Fluorescent Noncanonical Aminoacid Tagging*), our laboratory was able to show that newly synthesised proteins were mostly located at the cristae membranes [19]. We now report that further use of mitochondrial FUNCAT reveals a heterogeneous distribution of translation within the mitochondrial network in cultured cells, with a far greater level of synthesis occurring in the peri-nuclear region of the network as compared to the periphery after normalisation to mitochondrial mass. Quantification of mitoribosomal proteins (immunofluorescence) or mt-RNAs (RNA-FISH) confirms this mitochondrial protein synthesis gradient cannot completely be explained by a level of peri-nuclear enrichment of mitoribosome and mt-mRNA.

## 2. Materials and Methods

### 2.1. Cell Culture

Cultured dermal human fibroblasts, U2OS or HeLa cells were grown in Dulbecco's modified Eagle's medium, (Sigma D6429, Burlington, MA, USA) supplemented with 10% foetal calf serum (Sigma), 1× non-essential amino acids and 50 µg/mL uridine (Thermo

Fisher Scientific, Waltham, MA, USA) at 37 °C in humidified 5% CO<sub>2</sub>. Access to immortalised fibroblast lines originally derived from samples that were excess to diagnostic requirements were obtained according to the guidelines of the Declaration of Helsinki and approved by the Ethics Committee of Newcastle and North Tyneside Local Research (“Role of mitochondrial abnormalities in disease” REC ref 2002/205).

### 2.2. Fluorescent Non-Canonical Amino Acid Tagging (FUNCAT)

For FUNCAT experiments, cells were first seeded onto glass coverslips and cultured for 1–2 days. In vivo labelling of mitochondrial translation products was performed essentially as described [19]. Cells were pulsed (30 min, unless otherwise stated) with methionine-free DMEM containing the methionine analogue HPG (Jena Bioscience, Jena, Germany) with concomitant inhibition of cytosolic translation by cycloheximide (50 µg/mL). Cells were fixed before performing the copper-catalysed azide–alkyne cycloaddition of Alexa Fluor 594-picolyl-azide (CLK-1296-1) in a click chemistry reaction.

### 2.3. Immunofluorescent Cytochemistry

Specific mitochondrial targets of interest were co-labelled following 30 min of HPG and incorporation using primary antibodies diluted in 5% BSA for 1 hour at room temperature, followed by species-specific Alexa Fluor 532 (Thermo Fisher A11009 or A11002) or Alexa Fluor 594 (abcam ab150116 or Thermo Fisher A11012) diluted 1:200 in 5% BSA for 40 min. Nuclei were stained with Hoechst for 5 min and cells were mounted with ProLong Glass Antifade mountant. Primary antibodies used were TOM20 (Abcam, ab78547; Santa Cruz Biotechnology, SC-17764), mL45 (Protein Tech, PA5-54778), mS27 (Protein Tech, 17280-1-AP) and ATP5I (Protein Tech, 16483-1-AP).

### 2.4. RNA FISH/Immunofluorescent Cytochemistry

RNA FISH/IF was carried out as in Ref. [20] with minor modifications: Permeabilisation was carried out for 10 min, followed by incubation with respective antibodies (as above) in PBS. Stellaris Custom RNA FISH probe sets for rRNA and mRNA were designed with high stringency (masking level 5 and 4), respectively, using the Stellaris Designer tool (<https://www.biosearchtech.com/stellaris-designer>, accessed on 30 April 2021). Probe sets were purchased with either Quasar 570 or CAL Fluor 610 fluorophores from LGC Biosearch Technologies.

### 2.5. Confocal Imaging

Confocal imaging was performed on a Leica TCS SP8 (Leica Microsystems Mannheim, Germany) microscope equipped with white light lasers and HC PL APO 40×/1.30 Oil CS2 objectives for confocal imaging were used. The fluorophore Alexa Fluor 532 was excited at 527 nm and Alexa Fluor 594 was excited at 590 nm. Images were deconvolved using Huygens Essential, version 20.10 (Scientific Volume Imaging, Hilversum, The Netherlands).

### 2.6. Image Analysis

In each case, approximately 50 cells were analysed from a collective of three biologically repeated experiments. For characterising the colocalisation between mitochondrial markers, deconvolution and pixel-based colocalisation was applied (Scientific Volume Imaging). The colocalisation analysis utilised the non-parametric Spearman’s rank correlation coefficient to determine the correlation between fluorophore intensities, while Manders’ colocalisation coefficients (M1) were used to calculate proportions of co-occurrence between 0 and 1, which we have described in the text as a percentage with 1 equal to 100%. The means are given with 95% confidence intervals. To determine any significant differences between populations, the non-parametric paired Mann–Whitney U (Wilcoxon Rank Sum) Test was performed with a continuity correction where necessary as implemented in the `wilcox.test` function in R ([https://www.statskingdom.com/170median\\_mann\\_whitney.html](https://www.statskingdom.com/170median_mann_whitney.html), accessed on 5–6 August 2021).

### 3. Results

#### 3.1. Mitochondrial Translation Occurs Preferentially in the Peri-Nuclear Network

Initial data from mitochondrial FUNCAT visualising mitochondrial protein synthesis in fibroblasts, U2OS and HeLa cells had suggested an enrichment of translation in the peri-nuclear region of the cell compared to the periphery when normalised to a marker of mitochondrial mass [19]. To extend this analysis we subjected human cultured U2OS cells to mitochondrial FUNCAT as previously described [19,20]. All cell images were manually masked such that signals were assigned either to the peri-nuclear or peripheral regions of each cell. By quantifying the peri-nuclear and peripheral signals from a minimum of 50 cells and normalizing the signal to the mitochondrial marker TOM20, an outer membrane component of the protein import complex, we were able to show a distinct depletion of nascent protein synthesis towards the periphery of the cell (Figure 1A).

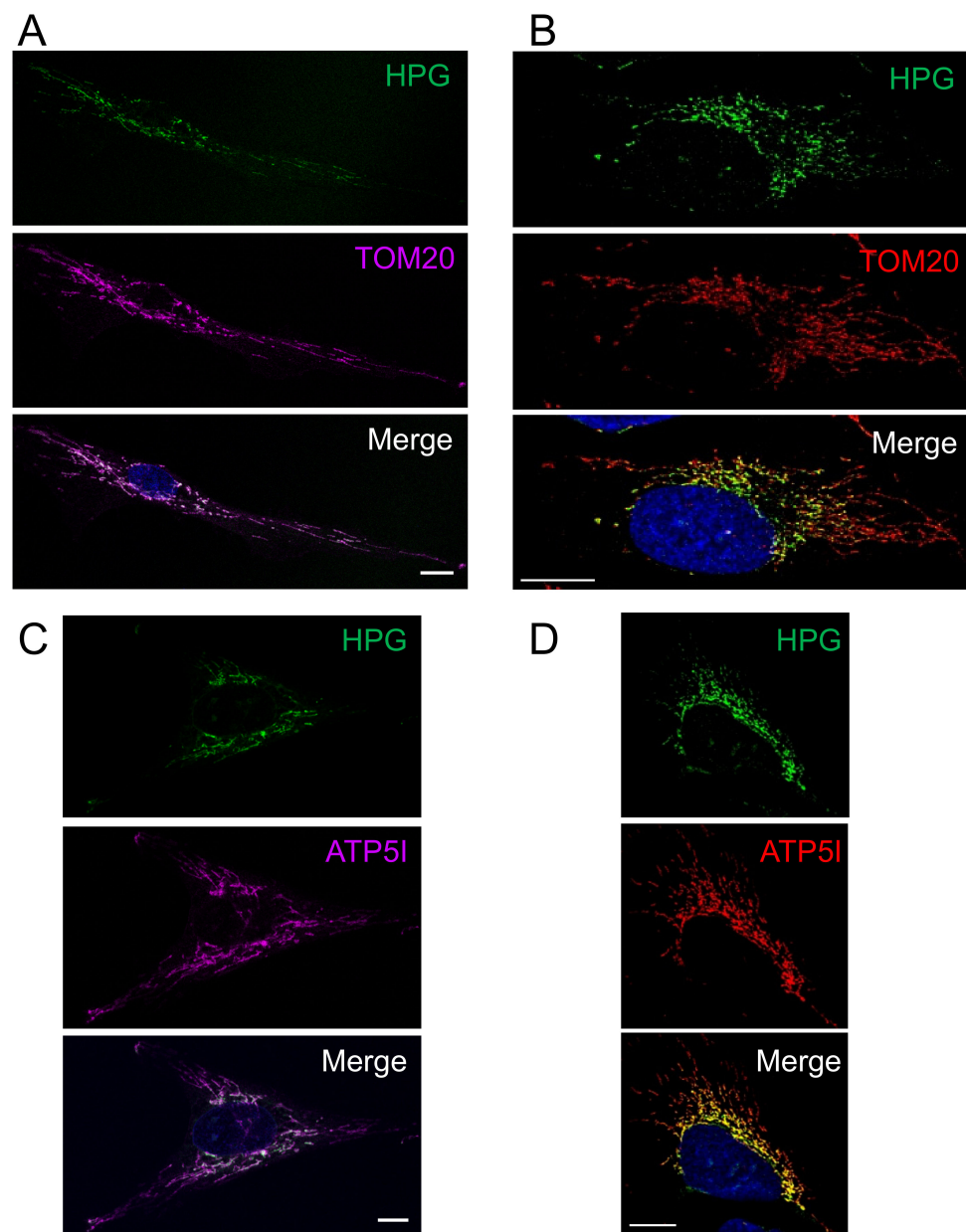


**Figure 1.** Preferential peri-nuclear mt-translation occurs in multiple cell types. Cells were pulsed with HPG for 30 mins in the presence of cycloheximide. Dermal fibroblast (A,C) and U2OS (B,D) cells were then fixed, click reactions performed and stained with antibodies against TOM20 (A,B) or ATP5I (C,D). Representative confocal images are shown. Scale bar = 10  $\mu$ m.

We wished to determine whether this marked intracellular gradient was a simple reflection of a similar gradient of the mature OXPHOS complexes. We chose to compare the pattern of synthesis with a marker, ATP5I, of the multi-subunit FoF1 ATP synthase that contains two mtDNA encoded components and is found mainly in the mitochondrial cristae, the infoldings of the mitochondrial inner membrane [21–23]. As shown in Figure 1B and quantified in Figure 4, a similar gradient of HPG signal diminishing towards the cell periphery is noted when compared to the immunofluorescent signal associated with ATP5I. These data confirm a strong concentration of mt-protein synthesis occurring preferentially within the peri-nuclear regions.

### 3.2. Preferential Peri-Nuclear Translation Is Not Reflective of a Similar Distribution of Mitoribosomes

The most likely explanation for this gradient in new protein synthesis across the mitochondrial network (Figure 2A) could simply be defined by a similar gradient in mitoribosome localisation. To address this possibility, confocal images were collected to facilitate comparison of the distribution of immunofluorescent signal of protein markers of the large (mL45, Figure 2B) and small (mS27, Figure 2C) mitoribosomal subunits. Similar normalisation to TOM20, as a marker of mitochondrial mass, reveals only a modest reduction in peripheral signal compared to the peri-nuclear signal for each of the mitoribosomal proteins (MRPs) (5% reduction for mL45 and 10% for mS27, compared to 55% reduction for HPG representing protein synthesis). To determine whether these values are artificially high as they represent a mixture of free (unassembled) MRPs or fully assembled mitoribosomes, we subjected cells to RNA FISH with probes specific to the ribosomal RNA components of the small (*RNR1*, Figure 2D) and large (*RNR2*, Figure 2E) mitoribosomal subunits.

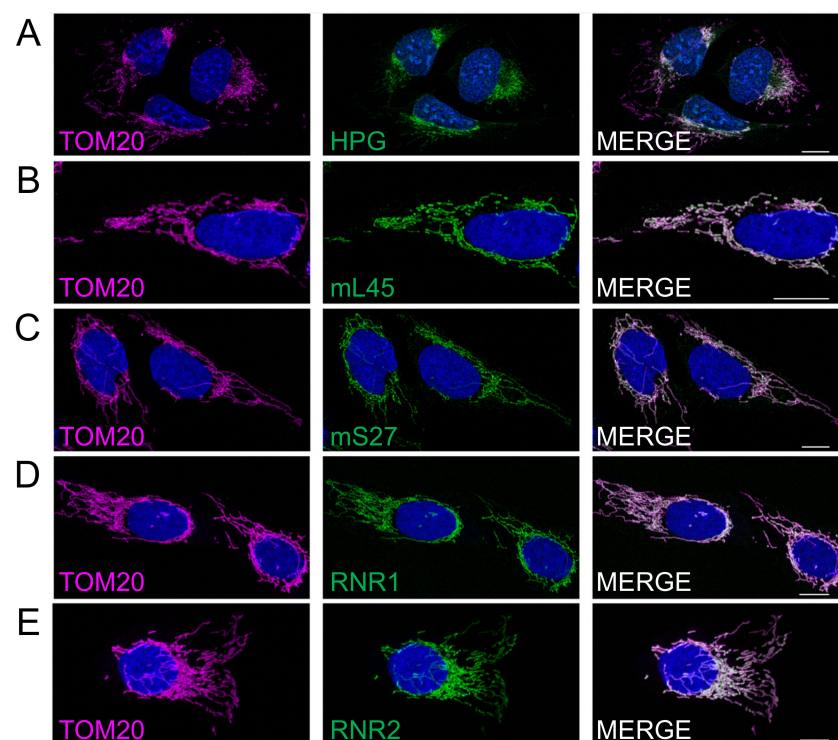


**Figure 2.** Mitoribosomal components show a different distribution to the HPG marker of mitochondrial translation. U2OS cells were immunostained with antibodies against TOM20 as a marker of the mitochondrial network either following HPG incubation and click chemistry (A) or co-stained with antibodies against mitoribosomal proteins of the large (mL45, panel B) or small (mS27, panel C) subunits. To determine the distribution of the RNA components of the small (*RNR1*, panel D) and large (*RNR2*, panel E) mitoribosomal subunits, immunostaining of TOM20 was combined with RNA FISH. Representative confocal images are shown. All scale bars = 10.01  $\mu\text{m}$ .

Quantification of images showed a similar reduction in the peripheral signal compared to the peri-nuclear signal for both the RNA and protein components of the small subunit (*RNR1* 18%, *mS27* 10%). However, a relatively greater reduction in signal was noted for the rRNA component of the mt-LSU, *RNR2* (26%) compared to *mL45* protein (5%). As it is highly likely that ribosomal RNA will not be stable in the absence of bound mitoribosomal proteins, the more marked reduction of the *RNR2* signal in the periphery as compared to an mt-LSU protein marker could reflect the presence of a subset of free *mL45* towards the periphery of the cell. Crucially, however, the decrease in peripheral signal noted for *RNR2* is still substantially less marked than for the HPG signal (26% decrease for *RNR2* cf. 55% decrease for HPG). Therefore, the extensive depletion in new protein synthesis that occurs in the peripheral mitochondrial network cannot be explained merely by a similar loss of mitoribosomes.

### 3.3. Differential Distribution of mt-Protein Synthesis Is Not Reflective of the mt-mRNA Distribution

As the diminished level of mitochondrial translation occurring in the peripheral mitochondrial network is not due to a paralleled loss of mitoribosomes, we next determined whether it could be explained by a lack of mt-mRNA available to load onto the mitoribosomes.

A similar protocol that had been used to visualise mitoribosomal rRNA by RNA FISH [20] was employed to detect the mt-mRNA that encodes COXII of complex IV. As shown in Figure 3A, once again there was a noticeable decrease in signal towards the periphery of the cell (35%) even after normalisation to the mitochondrial network marker TOM20. This depletion, however, was not comparable to the more extensive loss in the distribution of the HPG signal (35% cf. 55% Figure 3A vs. Figure 2A).

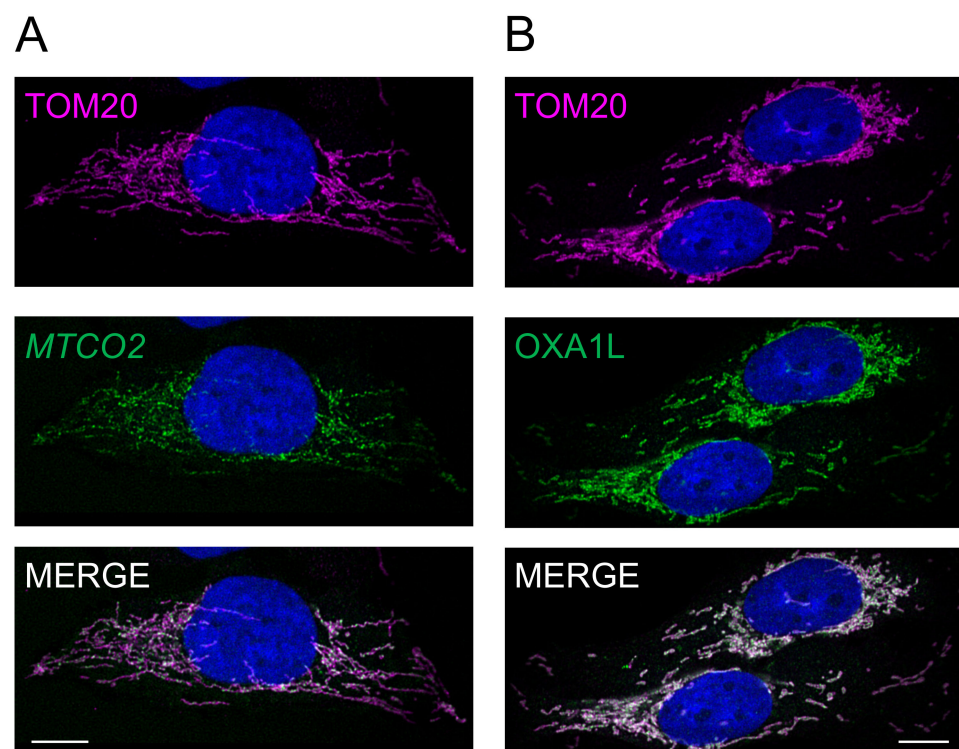


**Figure 3.** Neither transcript nor insertase levels appear to be limiting factors for mt-translation in peripheral regions of the reticulum. U2OS cells were immunostained with TOM20 antibodies to delineate the mitochondrial network either in combination with RNA FISH to define distribution of the mtDNA encoded *MTCO2* transcript (A) or co-stained with antibodies against the insertase *OXA1L* (B). Representative confocal images are shown. All scale bars = 10.06  $\mu\text{m}$ .

### 3.4. Peripheral Depletion of Mitochondrial Translation Cannot Be Explained by the Distribution of OXA1L

Although based solely on the use of the *MTCO2* RNA probe as an indicator of mt-mRNAs, it can be tentatively assumed that the decrease in translation is not correlated with a matching decrease in either mitoribosomes or in the availability of mt-mRNAs. What could be responsible for such a marked loss of translation in the peripheral mitochondrial network? The inner mitochondrial membrane insertase, OXA1L has for several years been implicated as a key player in facilitating insertion of the highly hydrophobic proteins encoded by mtDNA [24]. A more recent cryoEM study revealed how interactions between OXA1L and mL45 in the assembled mitoribosomes are able to couple protein synthesis to the insertion of the newly made protein into the inner membrane [25,26]. We, therefore, reasoned that the presence of OXA1L may dictate the distribution of newly translated protein. To determine whether or not the localisation of OXA1L was homogenous throughout the mitochondrial reticulum, we performed immunofluorescence with antibodies against OXA1L and TOM20 (Figure 3B).

Masking and quantification of these confocal images revealed that whilst the level of signal for OXA1L is reduced towards the periphery of the cell (28%), again it does not accurately track the loss of HPG signal (55%; Figure 4), establishing that this marked depletion in protein synthesis could not be entirely due to a lack of OXA1L.

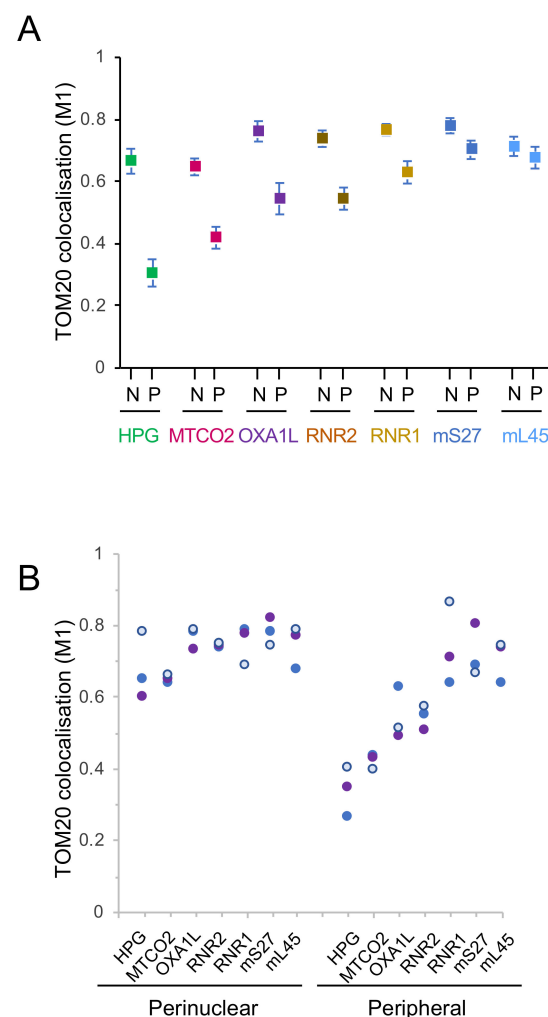


**Figure 4.** There is a differential distribution within the network of components involved in mitochondrial translation. In each case a minimum of 50 cells were analysed across three biological repeat experiments.

Following deconvolution, the correlation between fluorophore intensities of HPG ( $n = 54$ ), *MTCO2* ( $n = 50$ ), *RNR1* ( $n = 72$ ), *RNR2* ( $n = 77$ ), *mS27* ( $n = 59$ ), *mL45* ( $n = 54$ ), *Oxa1L* ( $n = 51$ ) normalised to TOM20 in both the peri-nuclear and peripheral regions was calculated using the Manders' colocalisation coefficient (M1) to determine relative co-occurrence. The mean and 95% confidence intervals are shown (A). The means (blue, white and purple circles) for each parameter are plotted to show the distribution of signal in the peri-nuclear versus peripheral regions for three biological repeats (B).

#### 4. Discussion

The focus of this mini-series is mitochondrial heterogeneity. Our data presented here and that of another recent publication [19] show clearly that for at least certain human cell lines there is evidence of marked heterogeneity in the location of translation within the mitochondrial network. Normalising mitochondrial signal using markers to either the outer mitochondrial membrane (TOM20) or the cristae membranes (FoF1 ATP synthase) confirm new protein synthesis is more markedly concentrated within the peri-nuclear mitochondrial network rather than towards the cell periphery. Interestingly, although we have normalised quantification of markers to the outer membrane marker TOM20, it is also known to show a gradient itself within the network, although clearly this is not as dramatic as the translation gradient [27]. A similar peri-nuclear enrichment had been originally claimed for mtDNA replication [28], but further studies involving careful normalisation to mitochondrial mass showed this was not the case [28,29]. To ensure our observations are robust, we have mapped the translation machinery through both the rRNA and protein components of the mitoribosome. We have looked at the localisation of a transcript (*MTCO2*) that is to be translated and the protein (*OXA1L*) that facilitates the insertion of the newly synthesised proteins into the inner mitochondrial membrane. Extensive colocalisation studies now show that this geographical heterogeneity of mt-protein synthesis is not the consequence of a similar distribution of mitoribosomal components nor of the localisation of mitochondrial mRNA, as the pattern for all these elements remains distinct from that of the HPG signal, which reflects the site of synthesis of mtDNA encoded proteins (Figure 4).

It is unclear what mechanism is responsible for this heterogeneity, or what might stimulate such variation. Perhaps the most likely explanation is that a gradient in the concentration of a key component(s) of mitochondrial translation is present across the cell or within the organelle. Due to the relatively rapid equilibration of soluble proteins, it is more difficult, although not impossible, to envision how such gradients of soluble factors involved in translation could be established. Thus, the integral membrane location of *OXA1L* together with its crucial membrane insertase role in mitochondrial protein synthesis made this a strong candidate. Although its partial peripheral depletion may explain part of the intracellular heterogeneity in mitochondrial translation it clearly cannot be the main underlying cause. What is the significance of such a gradient? A functional variation in the peri-nuclear and peripheral mitochondrial subpopulations was initially reported for the mitochondrial membrane potential, with the peripheral mitochondria being on average more hyperpolarised than the peri-nuclear fraction [30]. Consistent with this variation, peripheral mitochondria in several cell lines were shown to more rapidly clear agonist evoked  $\text{Ca}^{2+}$  flux from the cytosol [30]. Indeed, there are many examples of functional heterogeneity of mitochondria with respect to mitochondrial redox state, membrane potential, respiratory activity, uncoupling protein targeting and mitochondrial ROS production in cells both in vitro and in vivo (for review, see [31]). Nuclear gene expression has also been suggested to be modified by the accumulation of peri-nuclear mitochondria [32]. One additional possibility has recently been suggested by Lu et al. working with rabbit cardiac myocytes; the authors detailed a variety of functions that were markedly different in populations of subsarcolemmal, intrafibrillar or peri-nuclear mitochondria such as sensitivity to oxidative stress or maximal  $\text{Ca}^{2+}$  uptake [33]. Intriguingly, they also report a more rapid appearance of a mitochondrially-targeted GFP marker in the peri-nuclear compared to the other subcellular mitochondrial populations following viral transduction. This led to the suggestion that mitochondrial biogenesis may occur more readily in peri-nuclear mitochondria. A logical

extension would then be that new mitochondrial protein would then move out towards the periphery, where mitochondria would potentially be more stable. This model would be consistent with the observation that cells devoid of KIF5B, a key component in the intracellular movement of mitochondria, lose their peripheral mitochondria, which are suggested to be made via a process of dynamic tubulation of the peri-nuclear network [34]. Whilst it is a substantial extrapolation from data derived from cardiac myocytes to common human cell lines, the hypothesis that graded mitochondrial translation supports a model of graded mitochondrial biogenesis is intriguing and we expect to be able to test this soon.

## 5. Conclusions

Our studies confirm there is a marked gradient of mitochondrial translation across cultured human cells, with greater translation occurring in the peri-nuclear network. We have been able to show that this gradient is not due simply to a similar gradient of the mitoribosome or mitochondrial mRNA. Further, we also show this gradient is not due to a similar distribution of the inner membrane insertase OxalL. Potential explanations for this gradient are discussed.

**Author Contributions:** Conceptualisation, Z.M.C.-L., C.A.A., M.Z. and R.N.L.; Methodology, Z.M.C.-L., C.A.A., M.Z., R.B.-P. and R.N.L.; Formal analysis, Z.M.C.-L., C.A.A., M.Z. and R.N.L.; Investigation, C.A.A., M.Z., C.H., F.M., E.-A.S. and R.B.-P.; Writing—original draft preparation, Z.M.C.-L. and R.N.L.; Writing—review and editing, Z.M.C.-L., C.A.A., M.Z. and R.N.L.; Visualisation, Z.M.C.-L., C.A.A., M.Z. and R.N.L.; Supervision, Z.M.C.-L., C.A.A., M.Z. and R.N.L.; Project administration, Z.M.C.-L. and R.N.L.; Funding acquisition, Z.M.C.-L. and R.N.L. All authors have read and agreed to the published version of the manuscript.

**Funding:** This research was funded by The Wellcome Trust [203105/Z/16/Z] RNL and ZCL and the EU Marie Skłodowska-Curie ITN Grant No 721757) RNL and ZCL.

**Institutional Review Board Statement:** This was not a human study. Access to immortalised fibroblast lines originally derived from samples that were excess to diagnostic requirements were obtained according to the guidelines of the Declaration of Helsinki, and approved by the Ethics Committee of Newcastle and North Tyneside Local Research (“Role of mitochondrial abnormalities in disease” REC ref 2002/205).

**Informed Consent Statement:** Not applicable.

**Data Availability Statement:** The quantification of imaging data for perinuclear and peripheral regions of each cell presented in this study are openly available in the Newcastle University data repository at 10.25405/data.ncl.16810912.

**Conflicts of Interest:** The authors declare no conflict of interest. The funders had no role in the design of the study; in the collection, analyses, or interpretation of data; in the writing of the manuscript, or in the decision to publish the results.

## References

1. Adebayo, M.; Singh, S.; Singh, A.P.; Dasgupta, S. Mitochondrial fusion and fission: The fine-tune balance for cellular homeostasis. *FASEB J.* **2021**, *35*, e21620. [[CrossRef](#)]
2. Stoldt, S.; Wenzel, D.; Kehrein, K.; Riedel, D.; Ott, M.; Jakobs, S. Spatial orchestration of mitochondrial translation and OXPHOS complex assembly. *Nat. Cell Biol.* **2018**, *20*, 528–534. [[CrossRef](#)]
3. Ikon, N.; Ryan, R.O. Cardiolipin and mitochondrial cristae organization. *Biochim. Biophys. Acta Biomembr.* **2017**, *1859*, 1156–1163. [[CrossRef](#)] [[PubMed](#)]
4. Gilkerson, R.W.; Selker, J.M.; Capaldi, R.A. The cristal membrane of mitochondria is the principal site of oxidative phosphorylation. *FEBS Lett.* **2003**, *546*, 355–358. [[CrossRef](#)]
5. Stephan, T.; Bruser, C.; Deckers, M.; Steyer, A.M.; Balzarotti, F.; Barbot, M.; Behr, T.S.; Heim, G.; Hubner, W.; Ilgen, P.; et al. MICOS assembly controls mitochondrial inner membrane remodeling and crista junction redistribution to mediate cristae formation. *EMBO J.* **2020**, *39*, e104105. [[CrossRef](#)] [[PubMed](#)]
6. Wolf, D.M.; Segawa, M.; Kondadi, A.K.; Anand, R.; Bailey, S.T.; Reichert, A.S.; van der Bliet, A.M.; Shackelford, D.B.; Liesa, M.; Shrihari, O.S. Individual cristae within the same mitochondrion display different membrane potentials and are functionally independent. *EMBO J.* **2019**, *38*, e101056. [[CrossRef](#)] [[PubMed](#)]

7. Pearce, S.F.; Rebelo-Guiomar, P.; D'Souza, A.R.; Powell, C.A.; Van Haute, L.; Minczuk, M. Regulation of Mammalian Mitochondrial Gene Expression: Recent Advances. *Trends Biochem. Sci.* **2017**, *42*, 625–639. [[CrossRef](#)]
8. Kotrys, A.V.; Szczesny, R.J. Mitochondrial Gene Expression and Beyond—Novel Aspects of Cellular Physiology. *Cells* **2019**, *9*, 17. [[CrossRef](#)]
9. Garrido, N.; Griparic, L.; Jokitalo, E.; Wartiovaara, J.; van der Blik, A.M.; Spelbrink, J.N. Composition and dynamics of human mitochondrial nucleoids. *Mol. Biol. Cell* **2003**, *14*, 1583–1596. [[CrossRef](#)] [[PubMed](#)]
10. Feric, M.; Demarest, T.G.; Tian, J.; Croteau, D.L.; Bohr, V.A.; Misteli, T. Self-assembly of multi-component mitochondrial nucleoids via phase separation. *EMBO J.* **2021**, *40*, e107165. [[CrossRef](#)]
11. Satoh, M.; Kuroiwa, T. Organization of multiple nucleoids and DNA molecules in mitochondria of a human cell. *Exp. Cell Res.* **1991**, *196*, 137–140. [[CrossRef](#)]
12. Jourdain, A.A.; Koppen, M.; Wydro, M.; Rodley, C.D.; Lightowlers, R.N.; Chrzanowska-Lightowlers, Z.M.; Martinou, J.C. GRSF1 regulates RNA processing in mitochondrial RNA granules. *Cell Metab.* **2013**, *17*, 399–410. [[CrossRef](#)] [[PubMed](#)]
13. Antonicka, H.; Sasarman, F.; Nishimura, T.; Paupe, V.; Shoubbridge, E.A. The mitochondrial RNA-binding protein GRSF1 localizes to RNA granules and is required for posttranscriptional mitochondrial gene expression. *Cell Metab.* **2013**, *17*, 386–398. [[CrossRef](#)] [[PubMed](#)]
14. Iborra, F.J.; Kimura, H.; Cook, P.R. The functional organization of mitochondrial genomes in human cells. *BMC Biol.* **2004**, *2*, 9. [[CrossRef](#)] [[PubMed](#)]
15. Hensen, F.; Potter, A.; van Esveld, S.L.; Tarres-Sole, A.; Chakraborty, A.; Sola, M.; Spelbrink, J.N. Mitochondrial RNA granules are critically dependent on mtDNA replication factors Twinkle and mtSSB. *Nucleic Acids Res.* **2019**, *47*, 3680–3698. [[CrossRef](#)] [[PubMed](#)]
16. Anderson, S.; Bankier, A.T.; Barrell, B.G.; de Bruijn, M.H.; Coulson, A.R.; Drouin, J.; Eperon, I.C.; Nierlich, D.P.; Roe, B.A.; Sanger, F.; et al. Sequence and organization of the human mitochondrial genome. *Nature* **1981**, *290*, 457–465. [[CrossRef](#)]
17. Greber, B.J.; Bieri, P.; Leibundgut, M.; Leitner, A.; Aebersold, R.; Boehringer, D.; Ban, N. Ribosome. The complete structure of the 55S mammalian mitochondrial ribosome. *Science* **2015**, *348*, 303–308. [[CrossRef](#)]
18. Brown, A.; Amunts, A.; Bai, X.C.; Sugimoto, Y.; Edwards, P.C.; Murshudov, G.; Scheres, S.H.; Ramakrishnan, V. Structure of the large ribosomal subunit from human mitochondria. *Science* **2014**, *346*, 718–722. [[CrossRef](#)]
19. Zorkau, M.; Albus, C.A.; Berlinguer-Palmini, R.; Chrzanowska-Lightowlers, Z.M.A.; Lightowlers, R.N. High-resolution imaging reveals compartmentalization of mitochondrial protein synthesis in cultured human cells. *Proc. Natl. Acad. Sci. USA* **2021**, *118*. [[CrossRef](#)]
20. Zorkau, M.; Proctor-Kent, Y.; Berlinguer-Palmini, R.; Hamilton, A.; Chrzanowska-Lightowlers, Z.M.; Lightowlers, R.N. Visualizing Mitochondrial Ribosomal RNA and Mitochondrial Protein Synthesis in Human Cell Lines. *Methods Mol. Biol.* **2021**, *2192*, 159–181. [[CrossRef](#)]
21. Paumard, P.; Vaillier, J.; Couлары, B.; Schaeffer, J.; Soubannier, V.; Mueller, D.M.; Bredes, D.; di Rago, J.P.; Velours, J. The ATP synthase is involved in generating mitochondrial cristae morphology. *EMBO J.* **2002**, *21*, 221–230. [[CrossRef](#)]
22. Muhleip, A.; Kock Flygaard, R.; Ovcariakova, J.; Lacombe, A.; Fernandes, P.; Sheiner, L.; Amunts, A. ATP synthase hexamer assemblies shape cristae of Toxoplasma mitochondria. *Nat. Commun.* **2021**, *12*, 120. [[CrossRef](#)]
23. Davies, K.M.; Strauss, M.; Daum, B.; Kief, J.H.; Osiewacz, H.D.; Rycovska, A.; Zickermann, V.; Kuhlbrandt, W. Macromolecular organization of ATP synthase and complex I in whole mitochondria. *Proc. Natl. Acad. Sci. USA* **2011**, *108*, 14121–14126. [[CrossRef](#)]
24. Szyrach, G.; Ott, M.; Bonnefoy, N.; Neupert, W.; Herrmann, J.M. Ribosome binding to the Oxa1 complex facilitates co-translational protein insertion in mitochondria. *EMBO J.* **2003**, *22*, 6448–6457. [[CrossRef](#)] [[PubMed](#)]
25. Itoh, Y.; Andrell, J.; Choi, A.; Richter, U.; Maiti, P.; Best, R.B.; Barrientos, A.; Battersby, B.J.; Amunts, A. Mechanism of membrane-tethered mitochondrial protein synthesis. *Science* **2021**, *371*, 846–849. [[CrossRef](#)] [[PubMed](#)]
26. Desai, N.; Yang, H.; Chandrasekaran, V.; Kazi, R.; Minczuk, M.; Ramakrishnan, V. Elongational stalling activates mitoribosome-associated quality control. *Science* **2020**, *370*, 1105–1110. [[CrossRef](#)] [[PubMed](#)]
27. Wurm, C.A.; Neumann, D.; Lauterbach, M.A.; Harke, B.; Egnér, A.; Hell, S.W.; Jakobs, S. Nanoscale distribution of mitochondrial import receptor Tom20 is adjusted to cellular conditions and exhibits an inner-cellular gradient. *Proc. Natl. Acad. Sci. USA* **2011**, *108*, 13546–13551. [[CrossRef](#)] [[PubMed](#)]
28. Davis, A.F.; Clayton, D.A. In situ localization of mitochondrial DNA replication in intact mammalian cells. *J. Cell Biol.* **1996**, *135*, 883–893. [[CrossRef](#)] [[PubMed](#)]
29. Magnusson, J.; Orth, M.; Lestienne, P.; Taanman, J.W. Replication of mitochondrial DNA occurs throughout the mitochondria of cultured human cells. *Exp. Cell Res.* **2003**, *289*, 133–142. [[CrossRef](#)]
30. Collins, T.J.; Berridge, M.J.; Lipp, P.; Bootman, M.D. Mitochondria are morphologically and functionally heterogeneous within cells. *EMBO J.* **2002**, *21*, 1616–1627. [[CrossRef](#)]
31. Kuznetsov, A.V.; Margreiter, R. Heterogeneity of mitochondria and mitochondrial function within cells as another level of mitochondrial complexity. *Int. J. Mol. Sci.* **2009**, *10*, 1911–1929. [[CrossRef](#)]
32. Al-Mehdi, A.B.; Pastukh, V.M.; Swiger, B.M.; Reed, D.J.; Patel, M.R.; Bardwell, G.C.; Pastukh, V.V.; Alexeyev, M.F.; Gillespie, M.N. Perinuclear mitochondrial clustering creates an oxidant-rich nuclear domain required for hypoxia-induced transcription. *Sci. Signal.* **2012**, *5*, ra47. [[CrossRef](#)]
33. Lu, X.; Thai, P.N.; Lu, S.; Pu, J.; Bers, D.M. Intrafibrillar and perinuclear mitochondrial heterogeneity in adult cardiac myocytes. *J. Mol. Cell Cardiol.* **2019**, *136*, 72–84. [[CrossRef](#)]
34. Wang, C.; Du, W.; Su, Q.P.; Zhu, M.; Feng, P.; Li, Y.; Zhou, Y.; Mi, N.; Zhu, Y.; Jiang, D.; et al. Dynamic tubulation of mitochondria drives mitochondrial network formation. *Cell Res.* **2015**, *25*, 1108–1120. [[CrossRef](#)]